

## *Supplemental Information*

### **Supplemental Methods**

#### *Mice*

The subjects were young adult (2-4 months old) or old (18-20 months old) male C57BL/6J mice (Jackson Laboratory). Mice had free access to food and water and lights were maintained on a 12h light/dark cycle. All behavioral testing was performed during the light cycle. All experiments were conducted according to US National Institutes of Health guidelines for animal care and use and were approved by the Institutional Animal Care and Use Committee of the University of California, Irvine.

#### *Apparatus*

The OUL Updating paradigm was conducted in a set of four identical chambers (61 x 46 x 27 cm) constructed of opaque white Plexiglas. Each box had a strip of duct tape in the middle of one panel that served as an orienting mark. Additionally, the boxes were open to the room (i.e. not enclosed within a curtain) so that mice could use extra-maze cues for orientation. Boxes and objects were cleaned with 70% ethanol at the end of each behavior day and 10% ethanol between groups. All sessions were videotaped for offline analysis of object exploration. All objects used in OUL were identical 200-mL tall-form glass beakers filled with cement.

#### *OUL Behavioral Procedure*

The Objects in Updated Locations (OUL) procedure consisted of handling, habituation, training, updating, and testing, although the specific procedures varied slightly based on the experiment. In all experiments, mice were handled for two minutes per day for four days

Kwapis et al.

followed by six consecutive days of habituation. During each habituation session, mice were placed in the training context in the absence of objects and allowed to explore for five minutes. One day after habitation, mice were trained with two identical objects in specific locations (called  $A_1$  and  $A_2$ ) in the habituated context. Mice were either given a single 10-minute training session (Figures 1 and 2) or were given three consecutive days of 10-minute training sessions (Figures 3 and 4).

24h after the final training session, mice were given a 5-minute update session in which mice were assigned to either the No Update condition or the Update condition. For the No Update group, mice were re-exposed to the objects in the same locations as training ( $A_1$  and  $A_2$ ). For the Update group, one of the objects was moved to a new location (called  $A_3$ ) in a counterbalanced fashion. The update used in OUL is identical to the test session of a typical object location memory (OLM) experiment [1-4] in which exploration of the moved object is compared to exploration of the unmoved object to assess memory for the original training session. As mice prefer novelty, memory for the training session is demonstrated by increased exploration of the object in a new location. Thus, in addition to updating the original memory, the update session allowed us to verify that animals learned the initial training information. Preference for the novel location was expressed as a discrimination index (DI):  $(t_{A3} - t_{A1}) / (t_{A3} + t_{A1}) \times 100\%$ , where  $t$  indicates the time spent exploring the designated object. For No Update animals, as no novel location was presented at training, the DI was calculated comparing  $A_1$  and  $A_2$  to ensure the animals did not prefer either familiar location.

Finally, mice were given a test session to assess memory for both the original training information and the updated information. During the 5-minute test session, mice were exposed to four identical objects: three objects in previously experienced locations  $A_1$ ,  $A_2$ ,  $A_3$ , and a fourth

Kwapis et al.

object in a novel location, called A<sub>4</sub>. Memory for the original training information was inferred by calculating a DI to compare exploration of the novel location A<sub>4</sub> to objects in the original training locations A<sub>1</sub>:  $DI = (t_{A4} - t_{A1}) / (t_{A4} + t_{A1}) \times 100\%$  and A<sub>2</sub>:  $DI = (t_{A4} - t_{A2}) / (t_{A4} + t_{A2}) \times 100\%$ . Memory for the updated information was inferred by calculating a DI to compare exploration of the novel location A<sub>4</sub> to the updated location A<sub>3</sub>:  $DI = (t_{A4} - t_{A3}) / (t_{A4} + t_{A3}) \times 100\%$ . For No Update animals, as both locations A<sub>3</sub> and A<sub>4</sub> were novel, the object in the bottom right was considered to be location A<sub>4</sub> for the DI calculation to ensure the animals did not preferentially explore either novel location.

For the catFISH experiment (Fig. 3), the updating session consisted of two discrete 5-minute events (“epochs”) separated by 20 minutes and mice were sacrificed immediately after the second epoch.

### ***Cannulation surgery***

Chronic cannulae targeting the dorsal hippocampus were implanted as previously described [5]. Briefly, mice were anesthetized with isoflurane (4% induction, maintained at 1.5-2.0%) and placed in a stereotaxic apparatus. Bilateral 22 gauge guide cannulae (Plastics One) were lowered at a rate of 0.2mm/15s to the final site (AP -1.7mm, ML ±1.2mm, DV – 1.5mm relative to bregma). Cannulae were secured to the skull with dental cement and stainless steel dummy cannulae were placed in the cannulae to prevent occlusion. Mice were given a recovery period of at least 7d before behavioral testing began.

The final three days of habituation were used to acclimate animals to the injection procedure. Following each round of habituation, the mice were removed from boxes and transported to the injection room. The infusion pump was activated to allow mice to habituate to

Kwapis et al.

its noise. During this time, each mouse was gently scruffed and the obdurators were removed from the cannulae and cleaned as necessary.

### ***Drug preparation and infusion***

All mice in Fig.2 received bilateral infusions of anisomycin (ANI) or vehicle (VEH) into the dorsal hippocampus (1.0uL/side) immediately after the update session. ANI (Tocris #1290) was dissolved in equimolar HCL (~36uL) and diluted with artificial cerebrospinal fluid (ACSF, Tocris #3525) to the final concentration of 125µg/µL. The pH was tested with litmus paper and adjusted as necessary with a small amount of NaOH to match the ACSF vehicle. This preparation has reliably been shown to produce a reduction of ~60% in protein synthesis without lesions [6].

Following the update session, mice were transported to the injection room, gently scruffed, and the dummy cannulae were removed. The injectors, which extended ~0.5mm beyond the cannulae, were inserted into the guide cannulae and 1.0uL of ANI or VEH was infused into each hemisphere at a rate of 0.5µL per minute. Previous work with these parameters indicates that an injection of this volume produces bilateral coverage of the dorsal hippocampus in areas CA1-CA3 and the upper blade of the dentate gyrus [1,6-8]. Injectors remained in place for 90s after infusion to allow for diffusion before the injectors were removed, dummy cannulae were replaced, and mice were returned to their homecages.

### ***Cannula placement histology***

To confirm cannulae placements, histology was performed as described previously [5,7,9]. Briefly, following behavioral testing, animals were killed with an overdose of sodium

Kwapis et al.

pentobarbital and transcardially perfused with PBS followed by 4% paraformaldehyde using a peristaltic perfusion pump. Brains were removed, post-fixed overnight at 4°C and transferred to 30% sucrose-PBS until they sunk for cryoprotection. Frozen 40µm sections from the dorsal hippocampus were mounted on slides, stained with cresyl violet, and cannulae placements were confirmed. Animals with injection sites outside of the dorsal hippocampus were excluded from analyses.

### ***Fluorescence in situ hybridization for catFISH***

For the catFISH experiments (Fig. 3 and Supplementary Fig. 2), mice were euthanized with cervical dislocation and brains were removed and flash-frozen in isopentane over dry ice. Mice were euthanized immediately after Epoch 2 (Fig. 3), at the designated timepoint after training (Supplementary Fig. 2), or served as home cage controls. Home cage controls were handled, habituated, and trained identically to the experimental groups (or just handled and habituated for Fig. 2) but received no behavioral experience on the sacrifice day. Home cage groups were sacrificed directly from their home cages between behavioral groups to establish a baseline level of IEG expression for comparison. 20µm coronal slices were collected throughout the dorsal hippocampus in a grouped manner so that each slide contained an approximately anatomically matched hippocampal section from one brain in each of the four experimental groups. Slides were stored at -80°C.

Fluorescence *in situ* hybridization (FISH) for *Arc* was conducted as previously described [10,11]. We amplified the full-length *Arc* from mouse hippocampal cDNA and cloned the product into the pGEM-9Zf plasmid (Promega). Digoxigenin (DIG)-labeled *Arc* antisense and sense riboprobes were generated from this plasmid using a commercial transcription kit

Kwapis et al.

(MaxiScript kit, ThermoFisher Scientific) and a premixed RNA labeling nucleotide mix containing DIG-labeled UTP (Roche). The DIG-labeled *Arc* antisense probe was hybridized with the tissue overnight (at least one slide was hybridized with a DIG-labeled *Arc* sense probe each round as a control). The following day, the probe was visualized with an anti-DIG-HRP conjugate (Sigma) and visualized with a Cy3 substrate kit (TSA Cy3 Kit, PerkinElmer). Nuclei were counterstained with DAPI to allow nuclear *Arc* to be differentiated from cytoplasmic *Arc*.

### ***CatFISH image acquisition and analysis***

Area CA1b of the dorsal hippocampus, an area known to be critical for object location memories [12], was imaged and analyzed in the current study using a Zeiss LSM700 confocal microscope with a 40X oil objective. The pinhole, gain, and exposure remained constant for all images collected for each slide, in which each of the four groups was represented. The settings were optimized for detecting both intranuclear *Arc* puncta and diffuse cytoplasmic *Arc* staining. Confocal z-stacks were collected from three slides per animal and the cells in dorsal hippocampus CA1b were counted bilaterally.

CatFISH was scored as previously described [10,11,13] by an experimenter blind to the behavioral conditions. Each image was displayed on a computer with the FIJI image processing package for ImageJ and the image was overlaid with a transparency. Each cell was circled and non-neuronal cells (small cells ~5 $\mu$ m in diameter with bright and uniform staining) were excluded from analysis [11,14,15]. Only neurons present in the middle ~20% of the stack were included in analyses and no partial cells were included. The neurons were then classified as either negative for *Arc*, positive for cytoplasmic *Arc* only, positive for nuclear *Arc* only, or positive for both cytoplasmic and nuclear *Arc*. As *Arc* expression is expressed in nuclear puncta

Kwapis et al.

within a few minutes of an event and expressed in the cytoplasm by ~20-30 minutes after an event, cytoplasmic *Arc* indicated the neuron was active during epoch 1 and nuclear *Arc* indicated the neuron was active during epoch 2, with both nuclear and cytoplasmic *Arc* expression indicating that the cell was active during both epochs.

CatFISH similarity scores were calculated as described in detail previously [11]. A perfect score of 1 indicates that an identical population of neurons was activated by both epochs. A score of 0 would indicate that an independent population of neurons was activated by each epoch.

### ***Statistical analysis***

Videos were manually scored offline to determine exploration time for the objects present during training, updating, or testing. All experimenters were blind to the group assignments when scoring. Behavior was scored as exploration when the animal's head was oriented toward the object within ~1cm or with the nose touching the object. Mice that showed a preference for one object on all days of training ( $DI > \pm 20$ ) were excluded from further analysis. Additionally, any mouse that explored the objects for less than 2s during the test session was removed.

Statistical analyses were performed using either two-tailed Student's *t*-tests, one-way ANOVAs or two-way ANOVAs followed by Sidak-corrected *t*-tests to compare individual groups. Mixed-model ANOVAs were used in instances in which one variable was a repeated measure (e.g. Fig. 3D, when comparing the subcompartmental distribution of *Arc* for each group). All statistics were performed with Graphpad Prism 7 software. Our analytic approaches are based on previously published work[1,4,8,16,17]. No statistical methods were used to predetermine sample sizes, but our sample sizes are similar to those generally used in the field,

Kwapis et al.

including those reported in previous publications[1,4,5,8,16]. Data distribution was assumed to be normal, with similar variance observed among groups, but this was not formally tested. Main effects and interactions for all ANOVAs are described in the text along with the specific number of animals used in each individual experiment. All analyses were two-tailed and required an  $\alpha$  value of 0.05 for significance. Data are all shown as mean  $\pm$ SEM. For all experiments, values  $\pm$ 2SD from the group mean were considered outliers and were removed from analyses.

### ***Data availability***

The data supporting the findings of this study are available from the corresponding author upon reasonable request.

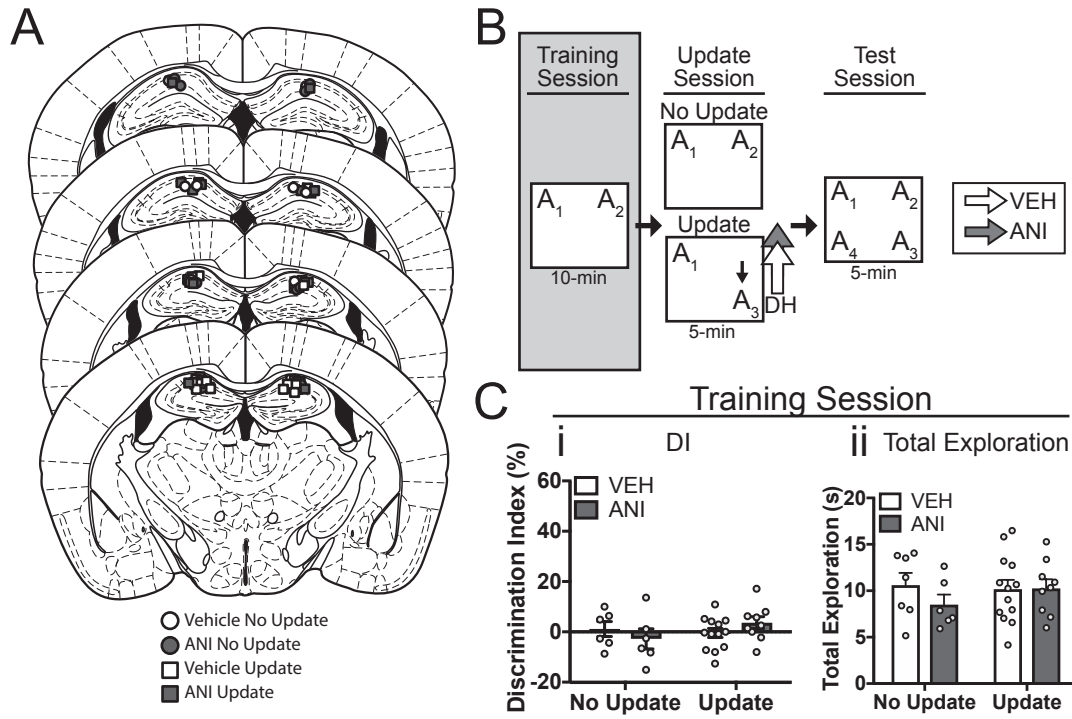


### Supplemental References

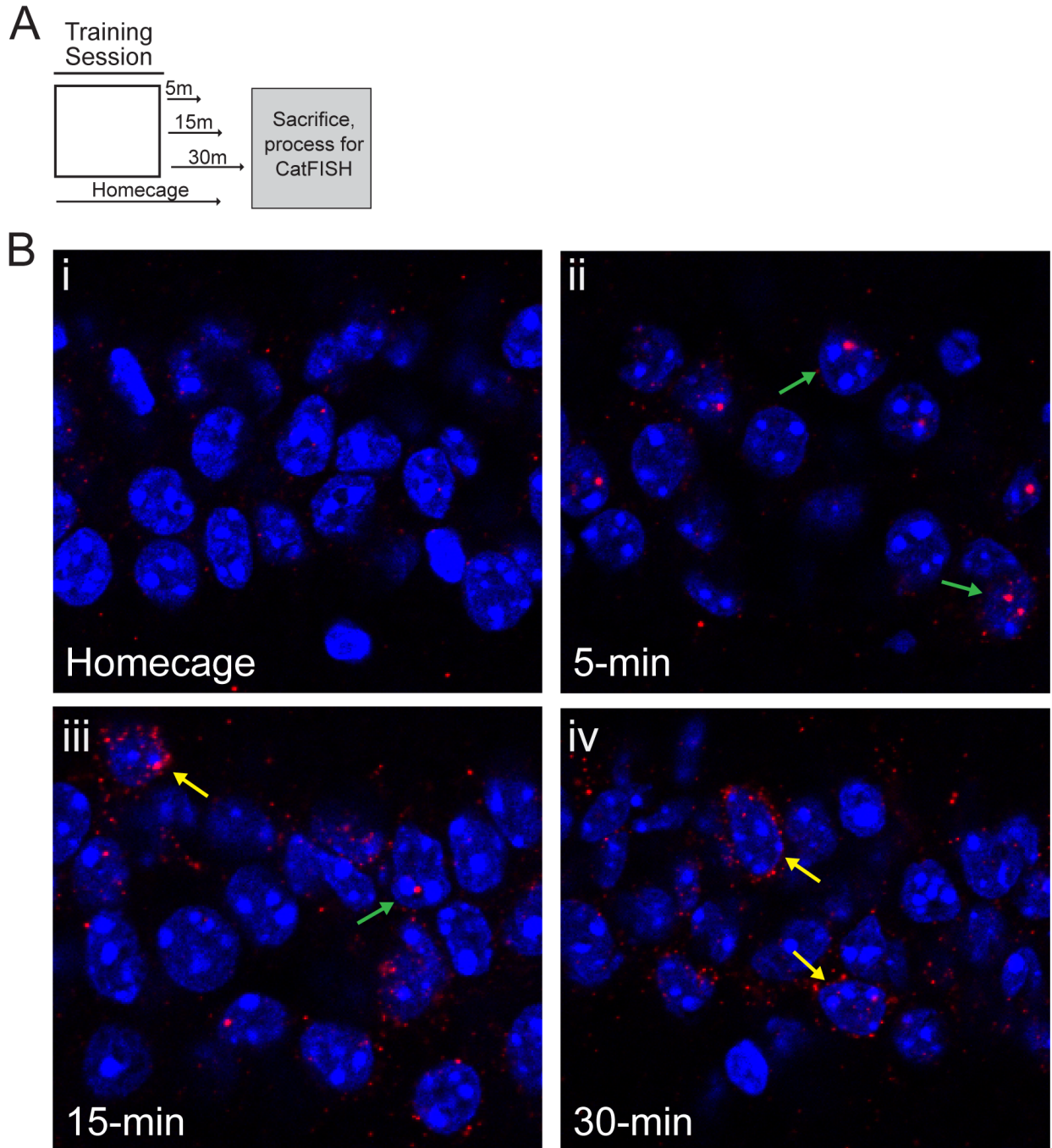
- 1 Kwapis JL, Alaghband Y, Kramar EA, Lopez AJ, Vogel Ciernia A, White AO, et al. Epigenetic regulation of the circadian gene *Per1* contributes to age-related changes in hippocampal memory. *Nat Commun.* 2018;9(1):3323.
- 2 Vogel-Ciernia A, Wood MA. Examining object location and object recognition memory in mice. *Current protocols in neuroscience.* 2014;69(8.31):1-17.
- 3 Alaghband Y, Kwapis JL, Lopez AJ, White AO, Aimiwu OV, Al-Kachak A, et al. Distinct roles for the deacetylase domain of HDAC3 in the hippocampus and medial prefrontal cortex in the formation and extinction of memory. *Neurobiol Learn Mem.* 2017;145:94-104.
- 4 Lopez AJ, Kramar E, Matheos DP, White AO, Kwapis J, Vogel-Ciernia A, et al. Promoter-Specific Effects of DREADD Modulation on Hippocampal Synaptic Plasticity and Memory Formation. *J Neurosci.* 2016;36(12):3588-99.
- 5 Haettig J, Stefanko DP, Multani ML, Figueroa DX, McQuown SC, Wood MA. HDAC inhibition modulates hippocampus-dependent long-term memory for object location in a CBP-dependent manner. *Learning & memory (Cold Spring Harbor, NY).* 2011;18(2):71-9.
- 6 Parsons RG, Gafford GM, Baruch DE, Riedner BA, Helmstetter FJ. Long-term stability of fear memory depends on the synthesis of protein but not mRNA in the amygdala. *Eur J Neurosci.* 2006;23(7):1853-9.
- 7 Kwapis JL, Jarome TJ, Schiff JC, Helmstetter FJ. Memory consolidation in both trace and delay fear conditioning is disrupted by intra-amygdala infusion of the protein

- synthesis inhibitor anisomycin. *Learning & memory* (Cold Spring Harbor, NY). 2011;18(11):728-32.
- 8 Kwapis JL, Alagband Y, Lopez AJ, White AO, Campbell RR, Dang RT, et al. Context and Auditory Fear are Differentially Regulated by HDAC3 Activity in the Lateral and Basal Subnuclei of the Amygdala. *Neuropsychopharmacology : official publication of the American College of Neuropsychopharmacology*. 2017;42(6):1284-94.
- 9 Kwapis JL, Jarome TJ, Gilmartin MR, Helmstetter FJ. Intra-amygdala infusion of the protein kinase Mzeta inhibitor ZIP disrupts foreground context fear memory. *Neurobiol Learn Mem*. 2012;98(2):148-53.
- 10 Guzowski JF, Worley PF. Cellular compartment analysis of temporal activity by fluorescence in situ hybridization (catFISH). *Current protocols in neuroscience*. 2001;Chapter 1:Unit 1.8.
- 11 Hartzell AL, Burke SN, Hoang LT, Lister JP, Rodriguez CN, Barnes CA. Transcription of the immediate-early gene *Arc* in CA1 of the hippocampus reveals activity differences along the proximodistal axis that are attenuated by advanced age. *J Neurosci*. 2013;33(8):3424-33.
- 12 Barrett RM, Malvaez M, Kramar E, Matheos DP, Arrizon A, Cabrera SM, et al. Hippocampal focal knockout of CBP affects specific histone modifications, long-term potentiation, and long-term memory. *Neuropsychopharmacology : official publication of the American College of Neuropsychopharmacology*. 2011;36(8):1545-56.
- 13 Guzowski JF, Setlow B, Wagner EK, McGaugh JL. Experience-dependent gene expression in the rat hippocampus after spatial learning: a comparison of the immediate-early genes *Arc*, *c-fos*, and *zif268*. *J Neurosci*. 2001;21(14):5089-98.

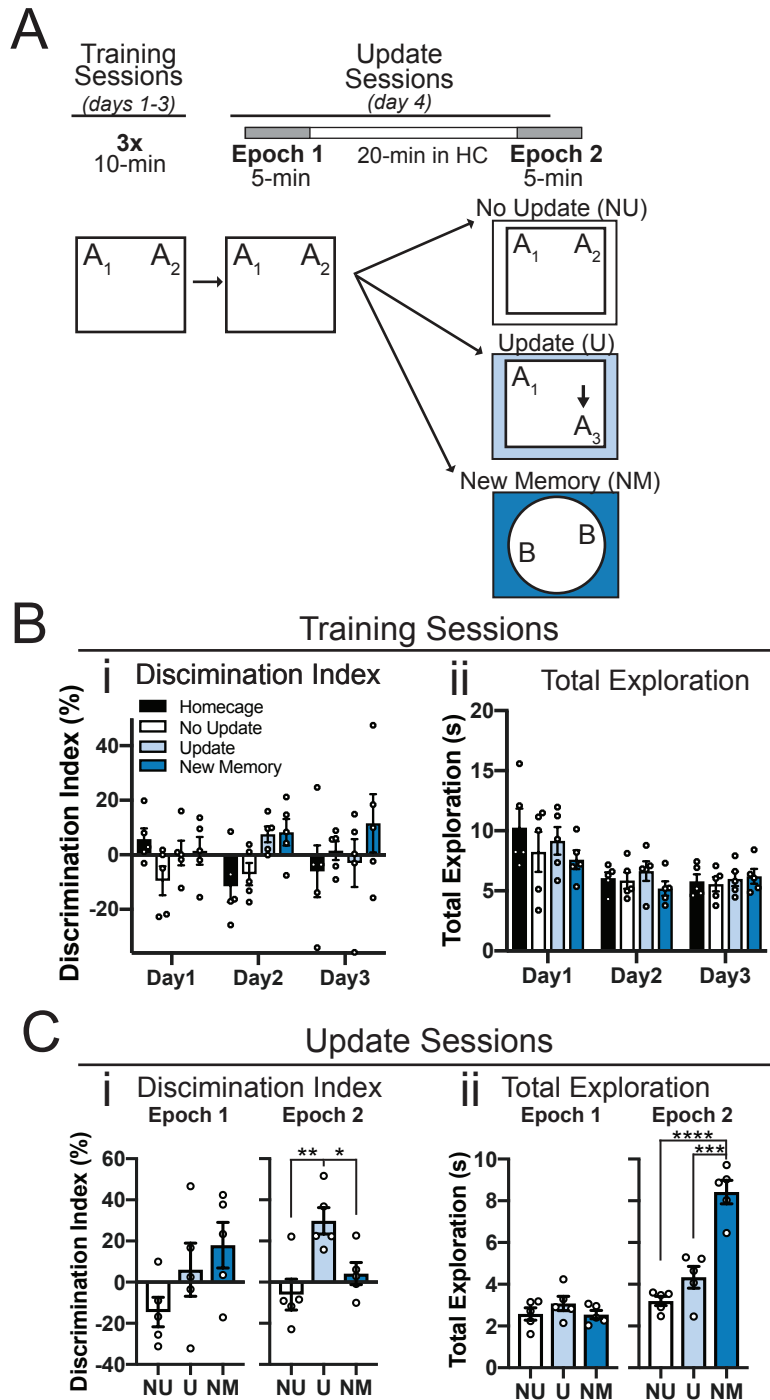
- 14 Vazdarjanova A, Guzowski JF. Differences in hippocampal neuronal population responses to modifications of an environmental context: evidence for distinct, yet complementary, functions of CA3 and CA1 ensembles. *J Neurosci.* 2004;24(29):6489-96.
- 15 Vazdarjanova A, McNaughton BL, Barnes CA, Worley PF, Guzowski JF. Experience-dependent coincident expression of the effector immediate-early genes *arc* and *Homer 1a* in hippocampal and neocortical neuronal networks. *J Neurosci.* 2002;22(23):10067-71.
- 16 Vogel-Ciernia A, Matheos DP, Barrett RM, Kramar EA, Azzawi S, Chen Y, et al. The neuron-specific chromatin regulatory subunit BAF53b is necessary for synaptic plasticity and memory. *Nat Neurosci.* 2013;16(5):552-61.
- 17 White AO, Kramar EA, Lopez AJ, Kwapis JL, Doan J, Saldana D, et al. BDNF rescues BAF53b-dependent synaptic plasticity and cocaine-associated memory in the nucleus accumbens. *Nat Commun.* 2016;7:11725.



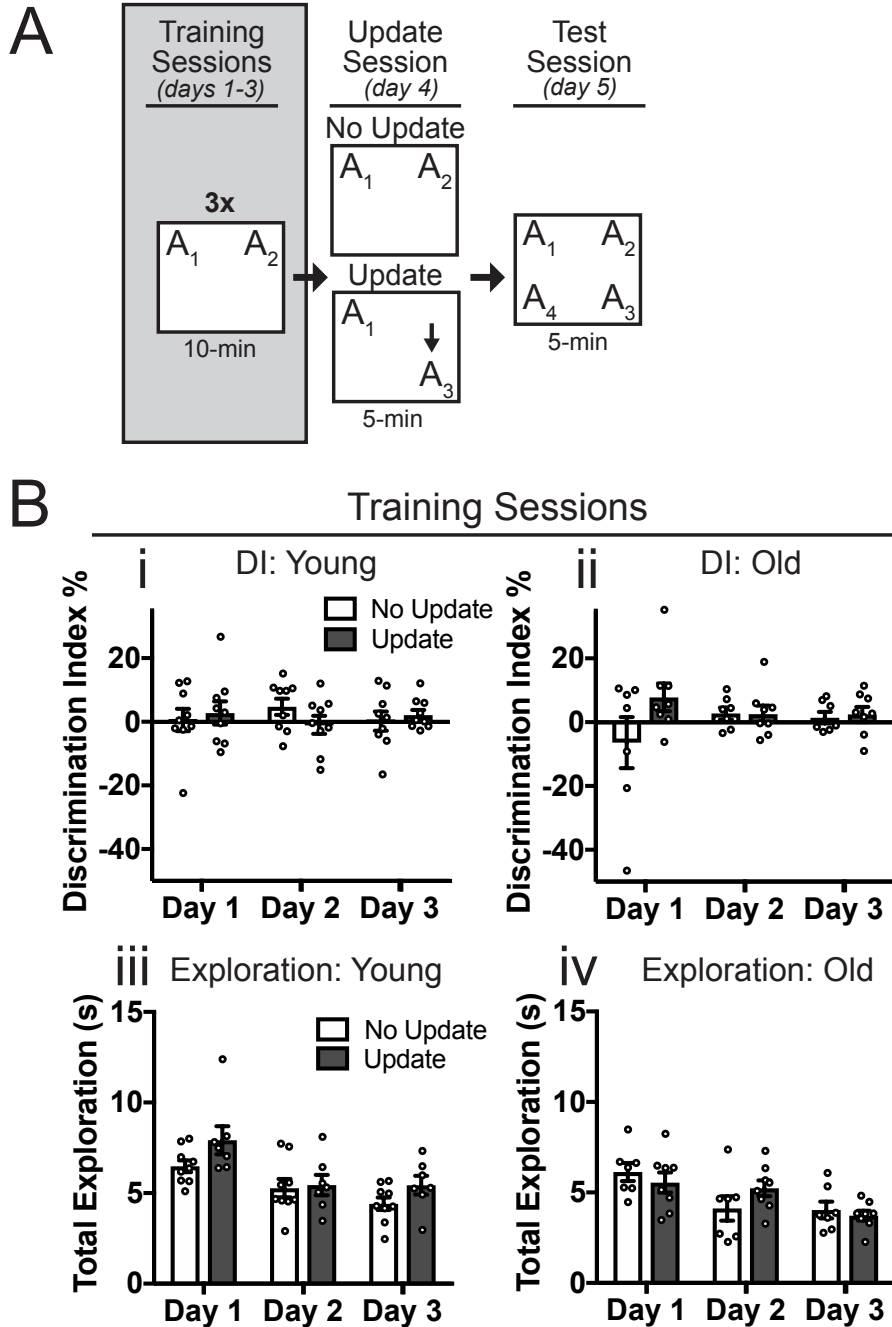
**Supplementary Figure 1.** Mice in Figure 2 do not prefer either object during training. **A)** Cannulae placements for all mice in Figure 2. Data are presented as mean  $\pm$ SEM. **B)** Experimental design. **C)** Training behavior. **i)** DIs were similar for locations A1 and A2 during training. **ii)** Mice showed similar total exploration across groups.



**Supplementary Figure 2.** *Arc* mRNA (red) is expressed in nuclear puncta five minutes after training and as cytoplasmic staining by 30 minutes after training. **A)** Experimental design. **B)** Example images from homecage mice (**i**) and mice sacrificed five minutes (**ii**), 15 minutes (**iii**), and 30 minutes (**iv**) after training. Green arrows: punctate nuclear staining. Yellow arrows: cytoplasmic staining. Nuclei are counterstained with DAPI (blue).

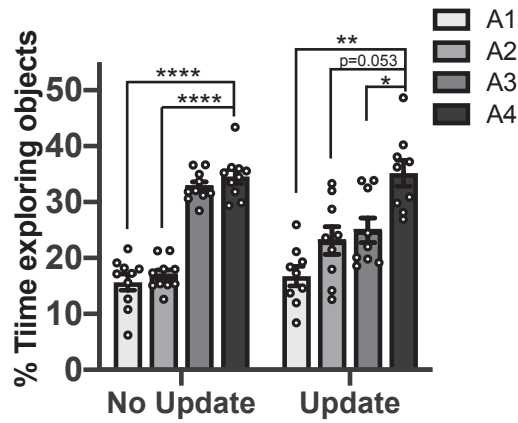


**Supplementary Figure 3.** Behavior for mice used in Figure 3 for CatFISH analysis. A) Experimental design. B) Training behavior. i) DIs were similar for locations A1 and A2 during training. ii) All groups showed similar levels of total exploration within each day of training. C) Behavior during the update session epochs. i) DIs were similar during Epoch 1, when all groups were exposed to the training locations. During Epoch 2, mice given the update (U) preferred the novel object location A<sub>3</sub> over the familiar location A<sub>1</sub> whereas No Update (NU) and New Memory (NM) mice show a DI near zero, indicating no preference. ii) Total exploration was similar for all groups during Epoch 1. During Epoch 2, mice in the New Memory group (exposed to a new context and novel objects) showed significantly more exploration than mice in the No Update or Update groups. Data are presented as mean ±SEM. \* $p < 0.05$ , \*\* $p < 0.01$ , \*\*\* $p < 0.001$ , \*\*\*\* $p < 0.0001$ .

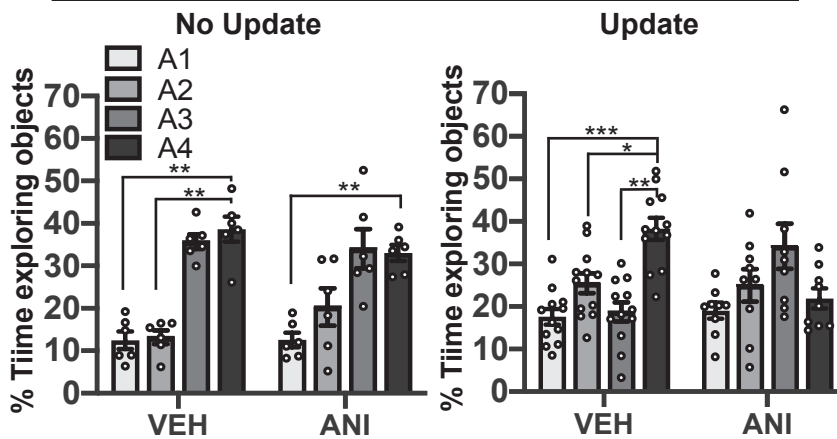


**Supplementary Figure 4.** Mice in Figure 4 do not prefer either object across the three days of training. **A)** Experimental design. **B)** Training behavior. **i-ii)** For young (**i**) and old (**ii**) mice, DIs were similar for locations A<sub>1</sub> and A<sub>2</sub> during training. **iii-iv)** Young (**iii**) and old (**iv**) mice showed similar total exploration across groups. Data are presented as mean  $\pm$ SEM.

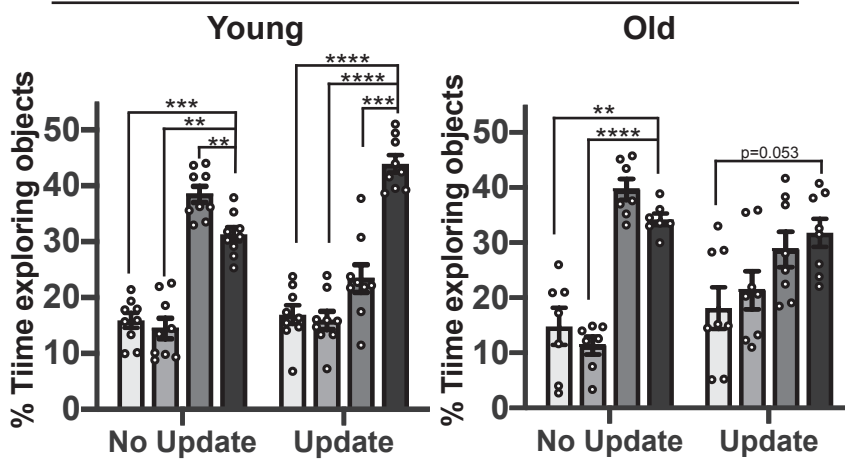
**A** Fig. 1 test (raw exploration)



**B** Fig. 2 test (raw exploration)



**C** Fig. 4 test (raw exploration)



**Supplementary Figure 5.** Raw object exploration time during test sessions (used to calculate DIs) for **A**) Fig. 1D. **B**) Fig. 2D **C**) Fig. 4C. All data were analyzed with two-way mixed model ANOVAs (repeated measure: Object, between-subjects measure: Drug or Update) followed by Dunnett's corrected posthoc tests comparing each object to A4. Data are presented as mean  $\pm$ SEM. \* $p < 0.05$ , \*\* $p < 0.01$ , \*\*\* $p < 0.001$ , \*\*\*\* $p < 0.0001$ .